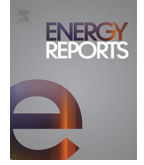




Available online at [www.sciencedirect.com](http://www.sciencedirect.com)

**ScienceDirect**

Energy Reports 8 (2022) 1172–1178



[www.elsevier.com/locate/egy](http://www.elsevier.com/locate/egy)

2021 8th International Conference on Power and Energy Systems Engineering (CPESE 2021),  
10–12 September 2021, Fukuoka, Japan

# A novel phase estimation method for renewable energy grid-connected equipments

Nanmu Hui\*, Xiaowei Han, Baoju Wu

*Institute of Scientific and Technological Innovation, Shenyang University, Shenyang 110044, China*

Received 25 October 2021; accepted 6 November 2021

Available online 26 November 2021

---

## Abstract

When renewable energy is applied to the power grid, it will cause problems such as harmonic interference and changes in grid frequency, resulting in harmonic distortion of the inverter and other renewable energy grid-connected equipments output current. So the grid-connected environment of weak grid puts forward higher requirements on the performance of phase-locked loop (PLL). Therefore, these renewable energy grid-connected equipments require Phase-Locked Loop (PLL) with higher technical performance. Aiming at the control requirements of inverter and other grid-connected equipments in weak grid, an optimization method based on a novel PLL is proposed. The method uses a dual enhanced novel cascade second-order generalized integrator (DENC SOGI) to simultaneously filter out the fundamental voltage negative sequence (FVNS) component and the DC offset (DCO) voltage component, and it can speed up the dynamic response and phase-locked accuracy of the PLL. The proposed PLL is verified by the simulation experiment platform. The performance of the approach is excellent and the grid-connected power quality of the renewable energy grid-connected equipments is guaranteed.

© 2021 The Author(s). Published by Elsevier Ltd. This is an open access article under the CC BY-NC-ND license (<http://creativecommons.org/licenses/by-nc-nd/4.0/>).

Peer-review under responsibility of the scientific committee of the 2021 8th International Conference on Power and Energy Systems Engineering, CPESE, 2021.

**Keywords:** Novel cascade second-order generalized integrator (NCSOGI); Enhanced novel cascade second-order generalized integrator (ENC SOGI); Phase-locked loop (PLL); Grid-connected inverter; DC offset (DCO)

---

## 1. Introduction

As the penetration rate of renewable energy power generation in the power grid continues to increase, the grid gradually exhibits the characteristics of a weak grid, and the resulting stability issues for grid-connected inverters have also received extensive attention in recent years. In the grid-connected inverter system, the phase-locked loop (PLL) is usually used to obtain the phase information of the grid voltage to ensure that the grid-connected current is synchronized with the grid voltage. Therefore, the performance of the phase-locked loop directly determines the stability of the grid-connected inverter [1,2].

---

\* Corresponding author.

E-mail address: [huinanmu@126.com](mailto:huinanmu@126.com) (N. Hui).

<https://doi.org/10.1016/j.egy.2021.11.085>

2352-4847/© 2021 The Author(s). Published by Elsevier Ltd. This is an open access article under the CC BY-NC-ND license (<http://creativecommons.org/licenses/by-nc-nd/4.0/>).

Peer-review under responsibility of the scientific committee of the 2021 8th International Conference on Power and Energy Systems Engineering, CPESE, 2021.

---

The grid synchronization method adopted by the existing grid-connected inverter mainly uses the PLL with fixed sampling time. Because of the fixed sampling time, this kind of methods can be consistent with the switching frequency of the inverter, which is convenient for analysis or design. The most commonly used method is synchronous reference frame PLL (SRF-PLL). To eliminate the interference of the asymmetric component of the input voltage on the SRF-PLL, the low-pass filter (LPF) usually be introduced for reducing the influence of the FVNS component in the grid synchronization process. However, the LPF reduces the bandwidth and the transient adjustment time of PLL. Therefore, a variety of improved filtering methods have emerged to replace the traditional LPF to improve the transient adjustment time of the PLL system. Jinming Xu [3] analyzed the stability of the system under the premise of considering the influence of the PLL, and pointed out that the phase-locked loop had a greater impact on the system characteristics within twice the bandwidth of the PLL, which may reduce the inverter system robustness in weak grid. The DDSOGIPNSC proposed by D. Prieto-Araujo [4] transforms the three-phase voltage by Clark, and then obtains its orthogonal signal by DDSOGI. According to the PNSC formula, the positive and negative sequence can be separated. The inverse Park transformation PNSC (IPT-PNSC) proposed by Daorong Lu [5] can be implemented in rotating coordinate system. It is similar to the PNSC based on  $\alpha\beta$  coordinate system, but the orthogonal signal generator is modified. Heng Nian [6] presented a novel symmetrical phase-locked loop. By modulating the  $d$ -axis and  $q$ -axis grid voltage signals at the same time, the system becomes a single input single output (SISO) system. Jinyu Wang [7] designed an impedance reshaping strategy, which significantly improved the stability margin of new energy power generation equipment in weak grid without affecting the reference signal tracking performance.

Aiming at the control requirements of grid-connected synchronization equipments in weak grid, this paper focuses on the improvement method of PLL in grid-connected inverter, uses the good filtering performance of DENC SOGI to suppress multiple harmonic components and to improve the transient adjustment performance and phase-locked accuracy of the system. By optimizing the dynamic performance of the PLL, the robustness of the grid-connected synchronization equipments will be improved. The simulation experiment platform for the PLL system is established to verify the effectiveness of the improved PLL in weak grid.

**2. Novel cascaded second-order generalized integrator design**

Since the FVNS component will have a serious impact on the phase-locked accuracy of the PLL, it is necessary to effectively filter out the FVNS component and accurately extract the fundamental voltage positive sequence (FVPS) component. For this purpose, a novel cascaded generalized second-order integrator (NCSOGI) is presented in this paper. Its structure is shown in Fig. 1.

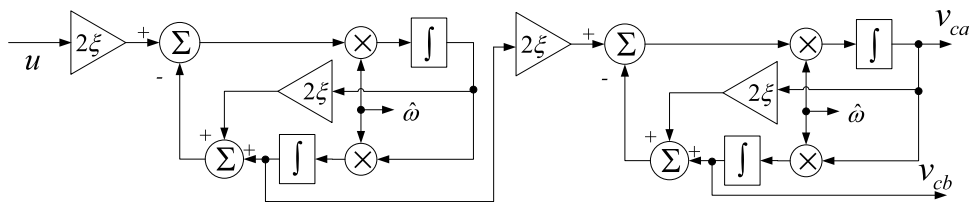


Fig. 1. The structure of NCSOGI.

Where, the input and output signal are  $u$  and  $v_{ca}$ ,  $v_{cb}$ , respectively, and  $\hat{\omega}$  is the estimated frequency. Through calculation, the transfer function of NCSOGI can be obtained as follows:

$$G_{ca}(s) = \frac{v_{ca}(s)}{u(s)} = \frac{4\xi^2\hat{\omega}^3s}{(s^2 + 2\xi\hat{\omega}s + \hat{\omega}^2)^2} \tag{1}$$

$$G_{cb}(s) = \frac{v_{cb}(s)}{u(s)} = \frac{4\xi^2\hat{\omega}^4}{(s^2 + 2\xi\hat{\omega}s + \hat{\omega}^2)^2} \tag{2}$$

According to Eq. (1),  $G_{ca}(s)$  has a zero point, which means that the transfer function of  $G_{ca}(s)$  has the function of rejecting DCO, that is, there is no DCO in  $v_{ca}$ . According to Eq. (2),  $G_{cb}(s)$  has no zero point, which means that the transfer function of  $G_{cb}(s)$  does not have the function of rejecting DCO, that is,  $v_{cb}$  will contain DCO. This will destroy the phase-locking accuracy of the phase-locked loop.

### 3. Enhanced novel cascaded second-order generalized integrator design

The implementation diagram of proposed enhanced novel cascaded second-order generalized integrator (ENC-SOGI) in this paper is shown in Fig. 2.  $v_{eb}$  is taken from another point in NCSOGI, so that  $v_{eb}$  does not contain DCO component.

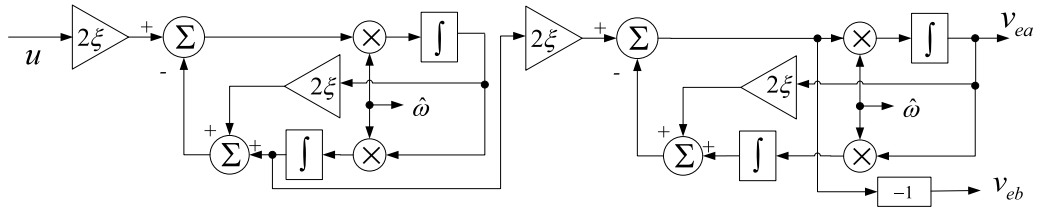


Fig. 2. The structure of ENC-SOGI.

In Fig. 2, the transfer function of ENC-SOGI can be derived as follow:

$$G_{ea}(s) = \frac{v_{ea}(s)}{u(s)} = \frac{4\xi^2 \hat{\omega}^3 s}{(s^2 + 2\xi \hat{\omega} s + \hat{\omega}^2)^2} \tag{3}$$

$$G_{eb}(s) = \frac{v_{eb}(s)}{u(s)} = -\frac{4\xi^2 \hat{\omega}^2 s^2}{(s^2 + 2\xi \hat{\omega} s + \hat{\omega}^2)^2} \tag{4}$$

According to Eq. (4), the numerator of  $G_{eb}(s)$  expression has two zero points, so the transfer function of  $G_{eb}(s)$  has the function of rejecting DCO. The expressions of  $G_{ea}(s)$  is the same as that of  $G_{ca}(s)$ , so  $v_{ea}$  does not contain the DCO component. Therefore, ENC-SOGI has the function of rejecting DCO, while NCSOGI does not have the function of rejecting DCO.

### 4. Proposed PLL based on DENC-SOGI

To ensure the accuracy of the phase and amplitude of the FVPS component extracted by the phase-locked loop, this paper adopts the interleaved structure of two ENC-SOGIs to propose the dual enhanced novel cascaded second-order generalized integrator (DENC-SOGI).

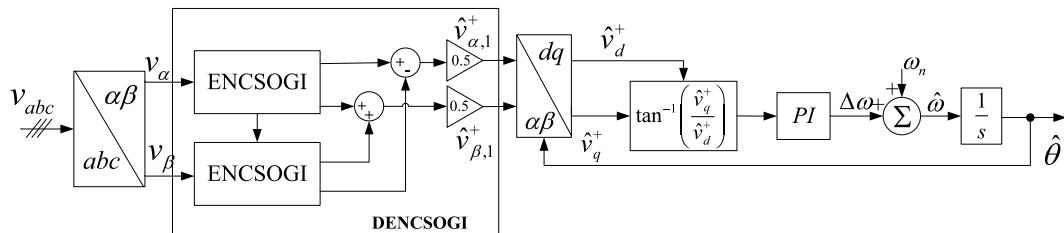


Fig. 3. The structure diagram of the proposed PLL based on DENC-SOGI.

Fig. 3 is the structure of the PLL based on DENC-SOGI proposed in this paper. The input–output relationship expression of DENC-SOGI can be obtained from Fig. 3 as follow:

$$\begin{bmatrix} \hat{v}_{\alpha,1}^+ \\ \hat{v}_{\beta,1}^+ \end{bmatrix} = \frac{1}{2} \begin{bmatrix} G_{ea}(s) & -G_{eb}(s) \\ G_{eb}(s) & G_{ea}(s) \end{bmatrix} \begin{bmatrix} v_{\alpha} \\ v_{\beta} \end{bmatrix} \tag{5}$$

In Eq. (5),  $v_{\alpha}$  and  $v_{\beta}$  are the input signals of DENC-SOGI in  $\alpha\beta$ -frame,  $\hat{v}_{\alpha,1}^+$  and  $\hat{v}_{\beta,1}^+$  are the output signals, and their expressions contain FFPS component.

According to the Ref. [8], DENC-SOGI is a complex filter with dual input and dual output structure, then the transfer function of the DENC-SOGI’s real and imaginary parts are

$$R_{DENC-SOGI}(s) = G_{ea}(s) = \frac{4\xi^2 \hat{\omega}^3 s}{(s^2 + 2\xi \hat{\omega} s + \hat{\omega}^2)^2} \tag{6}$$

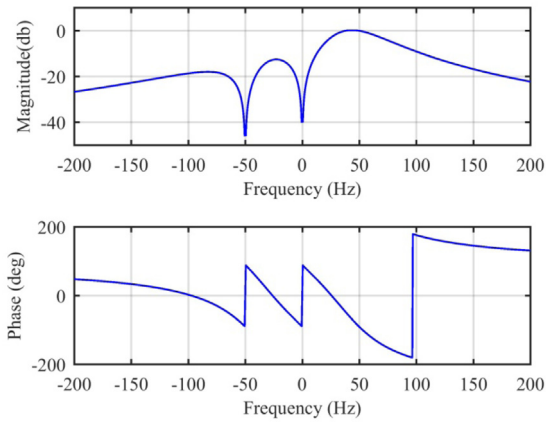


Fig. 4. Bode diagram of DENC SOGI(s).

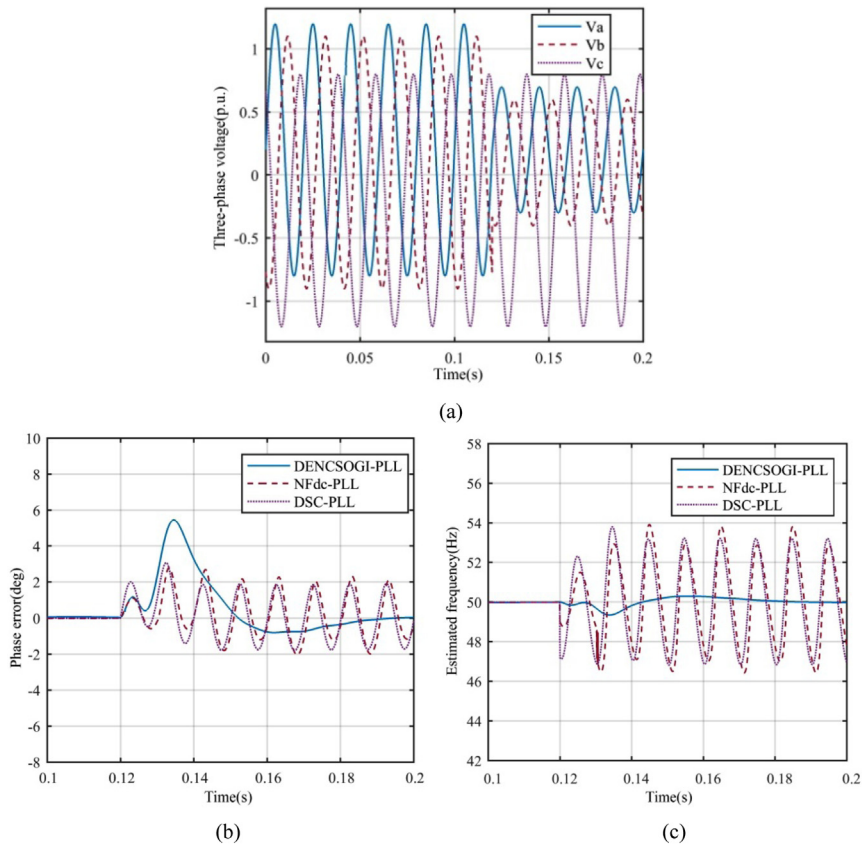


Fig. 5. The simulation test results under Case I, (a) voltage and (b) phase error and (c) estimated frequency.

$$Q_{DENC SOGI}(s) = G_{eb}(s) = -\frac{4\xi^2 \hat{\omega}^2 s^2}{(s^2 + 2\xi \hat{\omega} s + \hat{\omega}^2)^2} \tag{7}$$

According to Eqs. (5)–(7), the complex transfer function of DENC SOGI is

$$DENC SOGI(s) = \frac{1}{2}(R_{DENC SOGI}(s) + jQ_{DENC SOGI}(s))$$

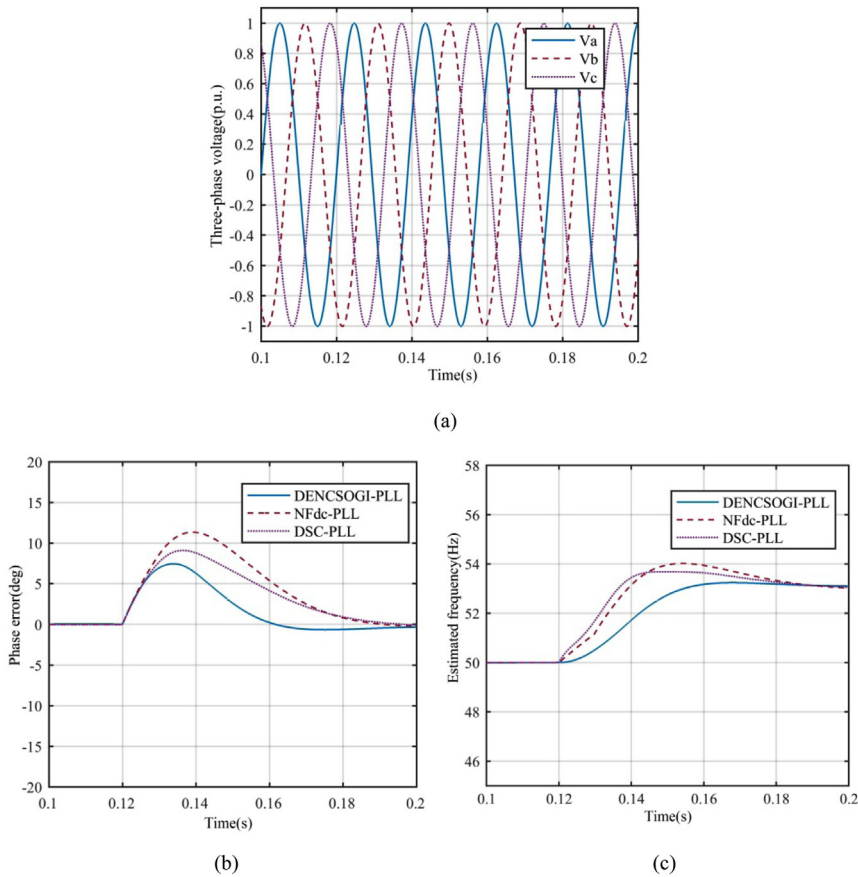


Fig. 6. The simulation test results under Case II, (a) voltage and (b) phase error and (c) estimated frequency.

$$= \frac{2\xi^2\hat{\omega}^3s - j2\xi^2\hat{\omega}^2s^2}{(s^2 + 2\xi\hat{\omega}s + \hat{\omega}^2)^2} \tag{8}$$

Fig. 4 is the bode plot of DENC SOGI(s), where  $\xi$  is 0.7.

It can be known from Ref. [9] that when the grid voltage is distorted and the grid frequency is 50 Hz, the value at  $-50$  Hz in  $\alpha\beta$ -frame is the FVNS component and the value at 0 Hz is the DCO component.

It can be observed from the above figure that in the  $\alpha\beta$ -frame, the magnification value of DENC SOGI(s) at  $-50$  Hz is  $-\infty$ , and the magnification value at 0 Hz is  $-\infty$ , which indicates that the FVNS and DCO can be rejected by DENC SOGI. At the grid frequency(50 Hz), the magnification value of DENC SOGI(s) is 0 and the corresponding phase is  $-90^\circ$ , so the DENC SOGI can accurately extract the FFPS component. The  $-90^\circ$  phase error can be corrected by  $90^\circ$  phase compensation.

### 5. Simulation experimental results

To verify the phase evaluation performance of DENC SOGI-PLL, the software MATLAB Simulink is used for simulation. The parameters based on DENC SOGI-PLL are: PI controller parameters  $k_p = 34.3$ ,  $k_i = 103.7$ , damping coefficient  $\xi = 0.707$ , input voltage amplitude  $U = 1$  p.u. (p.u. is voltage normalization value), frequency  $f = 50$  Hz. DENC SOGI-PLL is compared with two advanced PLLs with DCO cancellation function (including notch filter phase-locked loop (NF<sub>dc</sub>-PLL) [10] and delay signal cancellation phase-locked loop (DSC-PLL) [10]).

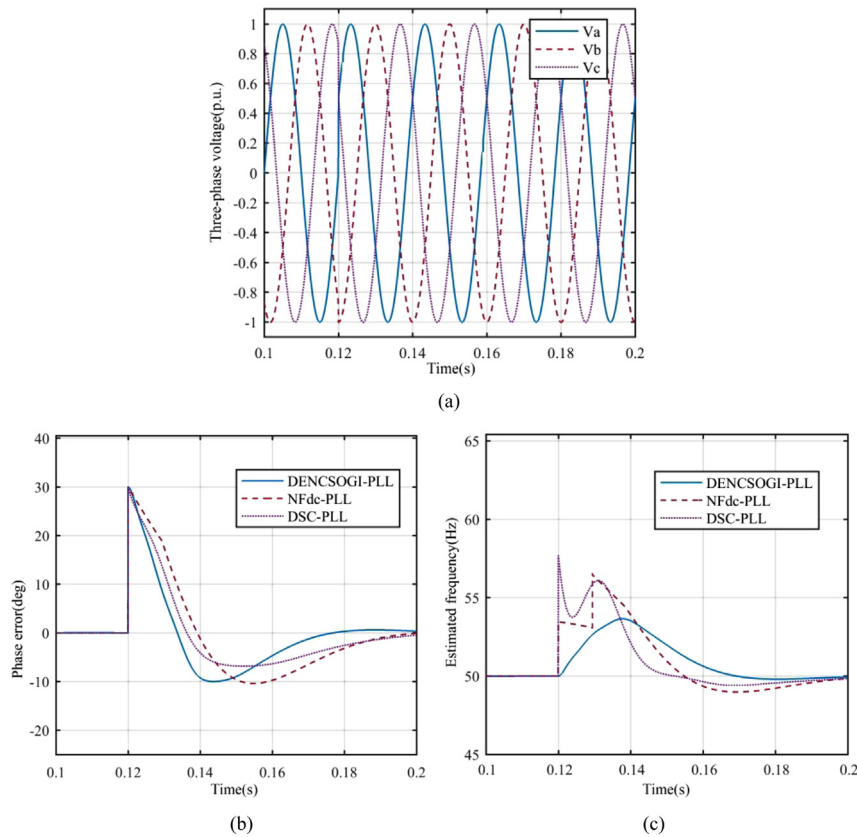


Fig. 7. The simulation test results under Case III, (a) voltage and (b) phase error and (c) estimated frequency.

### 5.1. Steady state characteristic test

To test the steady-state disturbance rejection performance of the proposed DENC SOGI-PLL, DCO disturbance and three-phase unbalanced voltage sag disturbance are injected into the grid voltage signal, the following test condition are adopted.

**Case I:** The DCO voltage is injected into the power grid at 0 s, which are 0.2 p.u., 0.1 p.u. and  $-0.2$  p.u. respectively. From 0.12 s, the three-phase unbalanced voltage drop disturbance is superimposed on the basis of three-phase voltage, specifically, the voltage fundamental waves of a and b phases fall to 0.5 p.u.

Fig. 5 shows the test waveforms of three PLLs under Case I. In this figure,  $NF_{dc}$ -PLL and DSC-PLL can no longer accurately track the phase angle and frequency of power grid under DCO and voltage sag interference, and the addition of DENC SOGI makes the proposed DENC SOGI-PLL achieve ideal steady-state tracking effect and zero steady-state error under DCO and voltage sag interference.

### 5.2. Dynamic characteristic test

To test the transient adjustment performance of the proposed DENC SOGI-PLL, the three-phase voltage signal is tested under the condition of frequency jump and phase angle jump. The following two test conditions are adopted.

**Case II:** 0-0.12 s is the three-phase sinusoidal balanced voltage of 50 Hz, and the instantaneous voltage frequency jumps to 53 Hz at 0.12 s.

Fig. 6 shows the test results of Case II. In the figure, under the frequency jump disturbance, the phase angle errors of the three PLLs can converge to zero after a short transient process, and the frequency can be accurately tracked after the transient process. In terms of rapidity, the proposed DENC SOGI-PLL has faster response speed than the other two PLLs, which verifies the good transient adjustment performance of the proposed control scheme.

**Case III:** 0-0.12 s is the three-phase sinusoidal balanced voltage of 50 Hz, and the voltage phase angle suddenly increases by  $30^\circ$  at 0.12 s.

Fig. 7 shows the test results of Case III. In this figure, after the phase angle jump occurs, the phase angle errors of the three PLLs can converge to zero in a short time, and the frequency can quickly recover the accurate tracking. In addition, we can also find that the transient curves of DENC SOGI-PLL are different from  $NF_{dc}$ -PLL and DSC-PLL. The proposed DENC SOGI-PLL has faster response speed and shorter stability time than the other two PLLs, which verifies the effectiveness of the proposed control scheme.

## 6. Conclusion

To solve the problem of instability of grid-connected equipments due to poor frequency and phase tracking performance of PLL under non-ideal weak grid, this paper proposes a DEDNCSOGI filtering method with FVNS component and DCO component rejection function. And an improved PLL is designed based on the DEDNCSOGI. The simulation experiment results show that the proposed PLL has faster dynamic response under weak grid conditions and has good robustness under complex disturbance.

## Declaration of competing interest

The authors declare that they have no known competing financial interests or personal relationships that could have appeared to influence the work reported in this paper.

## Acknowledgment

This work is supported by Natural Science Foundation of Liaoning Province, China (Grant No. 2020-BS-261) and Liaoning Provincial Department of Education Scientific Research Fund Project (Grant No. LJKZ1174).

## References

- [1] Venkatramanan D, John Vinod. Dynamic phasor modeling and stability analysis of SRF-PLL-based grid-tie inverter under islanded conditions. *IEEE Trans Ind Appl* 2020;56(2):1953–65.
- [2] Xin Chen, Yang Zhang, Shanshan Wang, Jie Chen, Chunying Gong. Impedance phased dynamic control method for grid-connected inverters in a weak grid. *IEEE Trans Power Electron* 2017;32(1):274–83.
- [3] Jinming Xu, Qiang Qian, Binfeng Zhang. Harmonics and stability analysis of single-phase grid-connected inverters in distributed power generation systems considering phase-locked loop impact. *IEEE Trans Sustain Energy* 2019;10(3):1470–80.
- [4] Eduardo Prieto-Araujo, Adrià Junyent-Ferré, Gerard Clariana-Colet, Oriol Gomis-Bellmunt. Control of modular multilevel converters under singular unbalanced voltage conditions with equal positive and negative sequence components. *IEEE Trans Power Syst* 2017;32(3):2131–41.
- [5] Daorong Lu, Jianxin Zhu, Jiangfeng Wang, Jianhui Yao, Sen Wang, Haibing Hu. A simple zero-sequence-voltage-based cluster voltage balancing control and the negative sequence current compensation region identification for star-connected cascaded H-bridge STATCOM. *IEEE Trans Power Electron* 2018;33(10):8376–87.
- [6] Heng Nian, Bin Hu, Xunyang Xu, Chao Wu, Liang Chen, Frede Blaabjerg. Analysis and reshaping on impedance characteristic of DFIG system based on symmetrical PLL. *IEEE Trans Power Electron* 2020;35(11):11720–30.
- [7] Jinyu Wang, Jun Liang, Feng Gao, Li Zhang, Zhuodi Wang. Symmetrical PLL for SISO impedance modeling and enhanced stability in weak grids. *IEEE Trans Power Electron* 2020;35(2):1473–83.
- [8] Yunlu Li, Dazhi Wang, Wei Han, Sen Tan, Xifeng Guo. Performance improvement of quasi-type-1 PLL by using a complex notch filter. *IEEE Access* 2016;4:6272–8.
- [9] Yunlu Li, Dazhi Wang, Yi Ning. DC-offset elimination method for grid synchronisation. *Electron Lett* 2017;53(5):335–7.
- [10] Saeed Golestan, Guerrero Josep M. Five approaches to deal with problem of DC offset in phase-locked loop algorithms: Design considerations and performance evaluations. *IEEE Trans Power Electron* 2016;31(1):648–61.